SLAC-PUB-12928
October 2007

Techniques of the FLASH Thin Target Experiment

Clive Field[1], Petra Huntemeyer[2] and Stanton Thomas[3]

For the FLASH Collaboration

[1] *Stanford Linear Accelerator Center, 2575 Sandhill Road, Menlo Park, CA 94025, U.S.A.*
[2] *Los Alamos National Laboratory, Los Alamos, NM 87545, U.S.A.*
[3] *University of Utah, Salt Lake City, UT84112, U.S.A.*

Submitted to Nuclear Instruments and Methods in Physics Research A

Work supported by the U.S. Department of Energy, Contract DE-AC02-76SF00515

Techniques of the FLASH Thin Target Experiment

Clive Field[1], Petra Hüntemeyer[2] *, and Stanton Thomas[3] for the FLASH Collaboration

[1] *Stanford Linear Accelerator Center, MS 62, 2575 Sand Hill Rd., Menlo Park, CA 94025, U.S.A*

[2] *Los Alamos National Laboratory, MS H803, Los Alamos, NM 87545, U.S.A*

[3] *University of Utah, Salt Lake City, UT 84112, U.S.A*

Abstract

The fluorescence yield in air is reported for wavelength and pressure ranges of interest to ultra-high energy cosmic ray detectors. A 28.5 GeV electron beam was used to excite the fluorescence. Central to the approach was the system calibration, using Rayleigh scattering of a nitrogen laser beam. In atmospheric pressure dry air, at 304 K, the yield is 20.8 ± 1.6 photons per MeV.

Key words: air fluorescence, fluorescence spectrum, ultra-high energy cosmic rays
PACS: 96.40.-z, 96.40.Pq, 98.70.Sa, 32.50.+d, 33.20.Lg

1. Introduction

As detector systems for ultra-high energy cosmic rays (UHECR) have become technically more advanced and statistically more powerful, one of the limiting sources of uncertainty has been in the knowledge of the physical processes used for the observations. In the case of modern telescope arrays, a critical process is fluorescence from air molecules, caused by UHECR shower formation in the atmosphere. In this paper, we describe improved techniques for measuring the fluorescence process in physical ranges applicable to the analysis of UHECR data.

There is a window of low sky-background light between approximately 300 and 400 nm. Telescope arrays use optical filters to monitor this range. Fortunately, within this window there is strong emission from the air fluorescence excited by cosmic rays. Emission is dominated by transitions within the nitrogen molecular band systems, near 315, 337, 355, 380 and 391 nm, with others of lesser intensity [1,2].

Several independent investigations of the fluorescence yield are proceeding and have produced results [3–8]. Among these, published yield measurements usually have been from experiments using sources, with relatively low electron energy. High resolution measurements of the full relevant spectrum have become available only recently. The profile of the light signal as a function of depth in actual multi-GeV electromagnetic showers has also been reported, with an indication that the spectrum is not sensitive to the depth in the shower [9].

One of the goals of the world-wide campaign to define the parameters of air fluorescence, has been to carry out measurements using technically different approaches. In this way, hidden difficulties would be uncovered, and greater confidence would be allowed in an eventual consensus on the results. The subject of this paper is the technique used in a set of measurements of the fluorescence yields of dry and moist air, reported in [10]. It covered the range of pressures relevant for UHECR showers. The experimental arrangement and calibration techniques are

* Corresponding author. *E-mail address*: petra@cosmic.utah.edu

systematically different from other approaches, and have allowed a substantial reduction in overall uncertainty.

2. Experimental Method

There were several differences between the techniques implemented in this work and other experiments. In the first place, a pulsed, high energy electron beam was used, where the majority of previously published electron-induced fluorescence measurements have used a radioactive source. Some advantages are that a) the monochromatic, penetrating, beam is easy to model, b) the fiducial light emission length is well defined, c) light signals can be strong, and statistics collected quickly, and d) photomultiplier dark counts are excluded by timing. A disadvantage is that stray radiation backgrounds must be reduced by shielding, and their remaining level must be monitored.

The FLASH (Fluorescence in Air from Showers) experiment was carried out at the Final Focus Test Beam (FFTB) facility at SLAC, operated at 28.5 GeV with pulses 3 ps long at 10 Hz. An air gap was provided in the beam vacuum line, with 50 micron thick stainless steel beam windows. The electron trajectories were effectively parallel, and the beam spot widths were typically ~ 1 mm.

Measurement of the FFTB beam intensity was improved substantially for the intensity range of this experiment. A beam toroid was coupled through a short cable to a purpose developed amplifier and bandpass filter [11], and sent outside the radiation enclosure for digitization on every beam pulse. By measuring the response to pulses of charge, on a wire simulating the electron beam, the calibration has been established with an uncertainty of 2.7%.

The fluorescence apparatus is illustrated in Fig. 1. The electron beam entered and left the gas volume through 25 micron aluminum pressure windows. The volume was a 25 cm long, 15 cm diameter cylinder. A pair of thin, blackened, aluminum tubes, 1.6 cm diameter, coaxial with the beam, and with a 1.67 cm gap between them, acted to define the measurement length for fluorescence light, while suppressing background from the forward-emitted Cherenkov light. There were two light channels, heavily baffled against scattered rays, extending radially from this gap. The pressure volume was terminated with 1.2 cm diameter fused silica windows, placed at 45 cm from the beam. This distance was

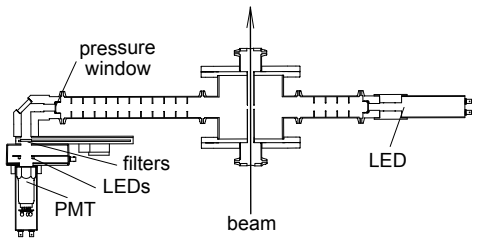

Fig. 1. The experimental setup.

as large as practical in order to eliminate Cherenkov light production in the fused silica. A right angle reflection, at a UV-enhanced aluminum-coated mirror, was then used before the light reached the photomultiplier tubes. This allowed the installation of heavy lead shielding to protect the tubes from radiation scattered directly from the beam.

In front of each PMT face was a remotely rotatable filter wheel with a sample of the filter material used in the HiRes telescopes, a thin opaque sheet used to study backgrounds, and a clear gap. In addition, there were narrow-band filters used for data still under study. Ultraviolet LEDs were used to help monitor stability in the photonics system. Four were placed in front of the PMT face, outside the fluorescence optical envelope. One was mounted on-axis, in a baffled tube diametrically opposite the light collection channel.

Enclosed in the same shielding as the active photomultipliers, were similar tubes with their photocathodes optically hooded. These were used as a continuous monitor of signals from radiation penetrating the shielding.

From outside the beam radiation enclosure, the system could be filled to a selected sub-atmospheric pressure with dry air, filtered moist air from the atmosphere, or, for systematic checks, with nitrogen which fluoresces much more strongly than air, or ethylene which fluoresces very weakly. The pressure settings used for data taking were in the range 10 to 750 torr.

3. Optical Calibration and Simulation

For the optical calibration, the thin target chamber (fully assembled) was installed in an environmental chamber in a laboratory at the University of Utah. Using a temperature controller the temperature in the environmental chamber was kept at the average temperature measured in the FFTB tunnel

at SLAC. A nitrogen laser [12] was mounted at a distance of approximately 2 m from the chamber. It injected a $\sim 160\mu$J beam pulse of 4 ns at a few Hz into the chamber along the electron beam axis. The light beam intensity was decreased by an aperture which was mounted on the beam port facing the laser. Thus the laser beam was confined to the center of the chamber and its size was similar to the size of the e^- beam. Because the Rayleigh scattering signal from air molecules is in the range of $\sim 10^{-6}$ of the beam, it is necessary to take great care to suppress any source of off-axis laser light. The scattered light passed through the baffled detector arms, was reflected by the UV enhanced aluminum coated mirror, passed through a filter or the clear gap in the filter wheel, and finally reached the PMT. The signals of the two photomultiplier tubes were digitized with the ADC system used at the FFTB. Simultaneously with the PMT signals, the energy of the outgoing laser beam was measured by a pyroelectric energy probe [13] installed on the opposite side of the chamber. The 25 mm diam. probe, suitable for pulsed beams of this type, had a calibration uncertainty of 5%, the largest individual contribution to the yield uncertainty. Based on Rayleigh scattering calculations as discussed in [14] and taking into account that fluorescence light is emitted isotropically, it then was possible to calculate the number of ADC counts per isotropically emitted 337 nm photon per meter. In order to be able to take measurements at different pressures inside the chamber, coated glass windows with close to 100% transmission efficiency in the UV range were attached to both beam ports. The thin target chamber was connected to a vacuum pump and a pressure gauge. Data were taken at several different pressures between vacuum and atmospheric pressure, and a linear fit,

$$\frac{N_{ADC} - N_{ped}}{E} = G \cdot \frac{SP}{T} + k_0 \qquad (1)$$

was performed to the data, varying the fit parameters G and k_0. Here, N_{ADC} is the signal counts recorded for each PMT, N_{ped} is the number of pedestal counts measured in the respective signal channel, E is the laser pulse energy, P, and T are the pressure and temperature measured in the chamber, and k_0 accounts for the light background from scattering of the laser beam with the chamber material. $S = 4.3 \cdot 10^7 \frac{photons}{m}$ is the expected Rayleigh scattering rate of 337.13 nm light calculated from the expressions in [14] for standard pressure (760 torr), and temperature (288.15 K). After the χ^2 minimization, G represents the calibrated number of ADC counts per isotropically emitted photon per meter at 337 nm. Data taken at twelve different pressure points for the clear aperture is displayed in Figure 2. It was found that the signal strength, normalized to the laser intensity, rose linearly with pressure, as expected from Rayleigh scattering. The intercept at the vacuum setting corresponded to the background from errant laser rays. The slope represents G.

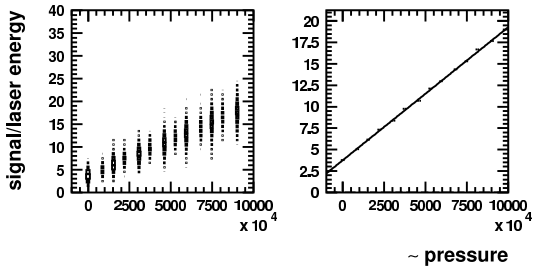

Fig. 2. PMT response against Rayleigh scattering intensity, controlled by changing air pressure. The plots represent equation 1. The left plot shows the scattering of the data during each of the pressure runs. The right plot shows the fit to the mean values of each run.

Because the detector was moved from the electron beam line to carry out laser studies, its light sensitivity was compared in both settings by using the built-in LEDs. Variations among the LEDs led to a significant uncertainty contribution of 2.5%, while possible thermal differences associated with radiation shielding contributed another 1.1%. Further systematic studies involved deriving the filter transmission efficiency of the HiRes filter at 337 nm from the Rayleigh scattering calibration of the setup with the clear aperture and the HiRes filter in place. The resulting difference in the calibration factors was compared to results from spectrophotometer measurements performed before the installation of the apparatus at SLAC. A systematic uncertainty of 1.8% has been assigned because of this filter consistency check. Finally, the fit shown in Fig. 2 was repeated while excluding the lowest pressure point. The resulting deviation from the original value of G was 0.2%.

Since the fluorescence light has a broad range of wavelengths, the system calibration must be extended at least over the ranges relevant to the PMT sensitivity and the HiRes filter material, approximately 300 - 420nm. This was performed by using a broad-band mercury lamp as a source for a monochromator, where the wavelength was selected with a precision of 0.5 nm. The light from the monochromator was monitored consecutively by

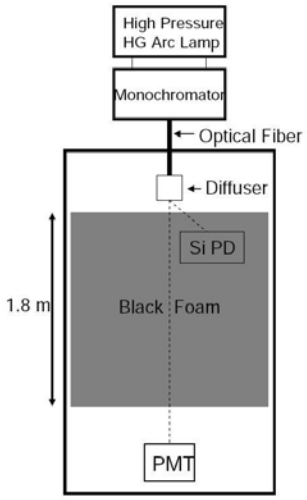

Fig. 3. The relative calibration setup. See text for details.

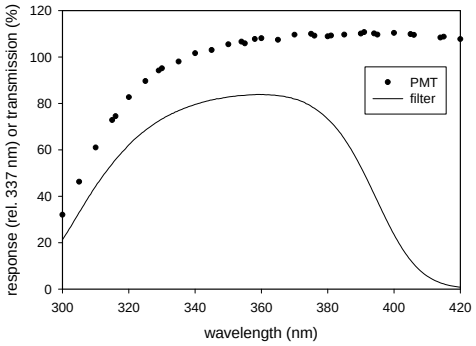

Fig. 4. PMT response relative to that at 337 nm, and transmission of HiRes filter, vs. wavelength.

two different close-by NIST wavelength-calibrated photodiodes (Si PDs) [15], and, at $\sim$ 200 cm distance, by the more sensitive PMT-filterwheel-UV-enhanced-mirror assembly. The setup is shown in Fig. 3. At each wavelength, many readings of current were averaged from the diodes and the PMT, and dark current was subtracted. In Fig. 4, the PMT response relative to that at 337 nm is shown, and may be compared with the transmission of the filter.

When calculating the overall sensitivity of the apparatus to the air fluorescence spectrum, allowance has been made for the small contributions beyond 420 nm by extending the sensitivity curve using manufacturer's data. The responses to two examples of measured spectra, from the Airfly collaboration [7] and from this experiment (see below), have been calculated, with good agreement.

In order to account for differences between the Rayleigh scattering, which is localized along the laser beam, and the electron beam energy deposit geometry, which has a diffuse tail extending centimeters from the beam line, further small corrections were applied. To evaluate these, the energy deposit geometry in the apparatus was simulated using EGS4 [16]. Using this, the overall acceptance efficiency at the optical iris was calculated numerically, and was compared with that for Rayleigh scattering from the laser beam using the same algorithm.

4. Analysis

Data were collected at selected settings of pressure, in runs of several thousand beam pulses. The digitized signals from the PMTs were corrected for zero-beam digitizer pedestals. With the help of opaque filter runs and the hooded counters, non-fluorescence backgrounds were subtracted. Only one of the light-channel PMTs was tuned for the wide band fluorescence yield measurement, and was used for this analysis. Even for this tube there was a non-linear behavior, and two separate effects were observed. The first was the familiar PMT saturation effect. It was significant in high light-signal nitrogen data. The more important effect, which applied also to the air data, was caused by electron beam pulses with high intensity. The strong, collective, radial electric field of the beam pulse accelerated electrons freed by ionization events, and thereby enhanced the deposited energy and fluorescence. The effect was removed from the data by applying beam intensity cuts, which were at 1.5×10^9 e^-/bunch at 1 atm, but had to be lowered for data at lower pressures, reaching 0.8×10^9 e^-/bunch at 50 torr. More information on calibration, simulation, and data processing can be found in [10]. Therein can be found also a more detailed description of the systematic uncertainties, which were studied and applied to the final result of the fluorescence yield. The various uncertainties are listed in Table 1 and sum up to an overall uncertainty of 7.5% which should be applied to the yield reported in the next section. Note that the three largest uncertainties come from the laser power measurement of the Rayleigh scattering calibration (5%), from the beam charge calibration (2.7%), and from the calibration transfer between the laboratory where the optical calibration was done and the beam line (2.5%).

Table 1
Uncertainty contributions on the photon yield in %.

Uncertainty	%
beam calibration	2.7
signal splitter	1.0
zero constraints of fits	1.0
run-to-run stability	1.0
laser vs e-beam light source shape	0.4
simulation	1.0
spectrum sensitivity, open filter	1.5
spectrum sensitivity, HiRes filter	1.0
beam line vs lab stability	2.5
2003 data calibration	2.0
PMT relative spectral response	1.2
Rayleigh scattering:	
laser power	5.0
filter consistency check	1.8
thermal sensitivity	1.1
theoretical calculations	0.2
fit slope	0.2
Sum	7.5

Table 2
Fluorescence yield between 300 and 600 nm. An overall uncertainty of 7.5% applies.

pressure (torr)	fluorescence yield	
	photons/MeV	photons/m/electron
760	20.8	5.059
495	32.0	5.029
242	64.3	4.848
97	157.6	4.686

5. Total Yield Results

The total photon yield in dry air is reported in Table 2, both in units of photons per MeV and photons per m per electron. There is agreement with previously published yields within the reported uncertainties [6,8,5], if we assume that the fluorescence signal increases with decreasing temperature $T \sim (1/P + b\sqrt{T/304})^{-1}$.

The yield was measured over a range of pressures. The initial rise with gas density was seen to saturate above ∼0.1 atm. This behavior is caused by increasing competition from molecular collision processes, principally involving oxygen.

Systematic checks were made by filling the apparatus with nitrogen and ethylene. The ratio of the fluorescence signal measured in nitrogen to that in dry air was found to be 6.51±0.37, and 6.84±0.29 for data collected with the clear aperture and the HiRes filter, respectively. This is in good agreement with the findings of [5] of 6.6±0.2. From measurements with ethylene at 750 torr an upper limit on the Cherenkov light contribution to the dry air signal of <0.21%, at 90% confidence, was placed.

Filtered air from outside the building, containing a relatively large fraction of water molecules, was also studied. For an overall pressure of 750 torr and 1.5% partial vapor pressure the light yield was found to be decreased by 7.4±0.3% with respect to the dry air case. For a pressure of 245 torr, the same fraction of water vapor decreased the light yield by a similar amount, $7.3 \pm 0.3\%$. By comparison, in the low temperature conditions at 5000 meters (400 torr), where much light from UHECR showers originates, the water vapor partial pressure saturates at 0.25%.

6. Spectrograph Results

The spectrum is needed in order to apply the calibration to actual fluorescence light, and also to calculate the wavelength-dependent opacity of the atmosphere caused by Rayleigh scattering. For this reason, it was studied [10] in a separate installation in the beam line. A compact spectrograph was employed to observe the important spectral lines simultaneously, rather than by a sequence of narrow band filters. Light from the vicinity of the beam passing through a gas enclosure was imaged on to the spectrograph slit. Once again, mirrors were employed to allow shielding against radiation. This avoided acceptance, and Cherenkov light background, issues associated with the use of optical fiber coupling to the spectrograph. The spectrum, covering $\sim 300 - 415$ nm, was measured by a 32-anode PMT. Backgrounds were measured by interrupting the light path before the spectrograph, and were very low.

Photonic calibrations were performed off the beam line. The wavelength settings were determined by using lines from a mercury discharge lamp, and the wavelength-dependent sensitivity was obtained by measuring the response to a deuterium lamp. There were some disadvantages in using the multianode PMT. A correction was necessary for saturation of the PMT response to the strongest lines. Also, smaller corrections were needed for

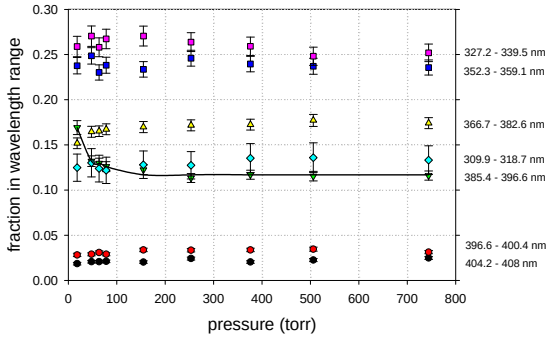

Fig. 5. Pressure variation of the relative contributions of various spectral ranges.

crosstalk between anode signals and non-uniformity of response near the edges of the anodes.

The detector sensitivity was found not to be very sensitive to spectrum details. In addition, the spectrum did not change substantially over the pressure range relevant for UHECR showers. This is illustrated in Fig. 5 where the lines are grouped into several wavelength bands. The very low pressure dominance of the 391 nm transition is expected [17].

7. Conclusion

The uncertainties of the present measurement have been reduced by a factor of about two with respect to the previous FLASH result [5]. This is mainly thanks to improvements in the beam charge calibration and the optical calibration. The total fluorescence yields presented in Table 2 of this paper are consistent with our previous result as well as with other yield measurements [6,8]. The agreement between the spectrum as measured by FLASH and those reported by Bunner [1], Nagano et al. [3], and the Airfly collaboration [7], is adequate for the data analyses of UHECR experiments at their present level of accuracy. This applies to both the detector sensitivity estimates and the Rayleigh-scattering loss calculations.

The calibration techniques described here can be developed to meet the demands of UHECR measurements as they become more stringent. Further developments on the beam toroid, including comparison with Faraday cup measurements, would be expected to reduce uncertainty contributions to the level of $\sim 1\%$. In situ detector calibrations, interspersed with electron beam data taking, would remove the system stability uncertainties, and the largest contribution, from the laser probe calibration, could be reduced to 2% with models now commercially available. With just these improvements, the overall uncertainty would be reduced to 4%.

We are indebted to the SLAC accelerator operations staff for their expertise in meeting the unusual beam requirements, and to personnel of the Experimental Facilities Department for very professional assistance in preparation and installation of the equipment. We also gratefully acknowledge the many contributions from the technical staffs of our home institutions. This work was supported in part by the U.S. Department of Energy under contract number DE-AC02-76SF00515 as well as by the National Science Foundation under awards NSF PHY-0245428, NSF PHY-0305516, NSF PHY-0307098, and NSF PHY-0400053.

References

[1] A.N. Bunner, Ph.D. Thesis, Cornell University (1967).
[2] G. Davidson and R. O'Neill, Jour. Chem. Phys 41 (1964) 3946.
[3] M. Nagano et al., Astropart. Phys. 20 (2003) 293; M. Nagano et al., Astropart. Phys. 22 (2004) 235.
[4] F. Kakimoto et al., Nucl. Instr. Meth. A 372 (1996) 527.
[5] J. Belz et al., Astropart. Phys. 25 (2006) 129.
[6] P. Colin et al., Astropart. Phys. 27 (2007) 317.
[7] M. Ave et al., Astropart. Phys. 28 (2007) 41.
[8] G. Lefeuvre et al., Nucl. Instr. Meth. A 578 (2007) 78.
[9] J. Belz et al., Astropart. Phys. 25 (2006) 57; P. Colin et al., arXiv:astro-ph/0703230v1, submitted to Elsevier Science.
[10] R. Abbasi et al., arXiv:astro-ph/0708.3116v1, submitted to Elsevier Science.
[11] Robert H. Simmons and Johnny S. T. Ng, Nucl. Instr. Meth. A 575 (2007) 334.
[12] Newport Corp., Mountain View, CA 94043; model VSL337ND-S.
[13] LaserProbe Inc., Utica, NY 13502; model RjP-734.
[14] A. Bucholtz, Appl. Opt. 34 (1995) 2765; B. Bodhaine et al., Oceanic Technol., 16 (1999) 1854; S. Chandrasekhar, *Radiative Transfer* (Dover, New York, 1960), Chap.1, p.49.
[15] Hamamatsu Photonics K.K., Shizuoka-ken 438-0193, Japan; model S2281.
[16] W. R. Nelson, H. Hiragama and D.W.O. Rogers, "The EGS4 Code System", SLAC-265, Stanford Linear Accelerator Center (1985).
[17] B. Keilhauer et al., Astropart. Phys. 25 (2006) 259.